Skeletal Radiology (2023) 52:1259–1262
https://doi.org/10.1007/s00256-023-04300-z

TEST YOURSELF: ANSWER

Test yourself answer: pain in the right hemithorax

Tatiana de Almeida Gonçalves Secco[1] · Walter Meohas[2] · Flavia Martins Costa[1,3] · Diogo Goulart Corrêa[3,4]

Received: 23 November 2022 / Revised: 3 January 2023 / Accepted: 31 January 2023 / Published online: 11 February 2023

Imaging presentation

Chest computed tomography (CT) showed an expansile lytic lesion, with no mineralized matrix, in the posterior portion of the right fourth rib, determining cortical erosion, with a lamellar, solid, and concentric periosteal reaction in this rib and in the adjacent third and fifth ribs, as well as pleural effusion (Fig. 1). Chest magnetic resonance imaging (MRI) showed the expansile lesion with isointense signal on T1-weighted imaging, predominantly hypointense signal on T2-weighted imaging, and hyperintense signal on short tau inversion recovery (STIR) relative to skeletal muscles, with avid gadolinium enhancement. Extensive edema in the adjacent bone marrow and soft tissues, as well as reactive pleural effusion, with avid gadolinium enhancement were also seen. There were signs of high perfusion in the lesion, as well as in the adjacent bone marrow, soft tissues, and pleural effusion. However, the time-signal intensity curve analysis demonstrated that the lesion presented an early, intense, and rapid enhancement, with washout, whereas the adjacent soft tissues edema and reactive pleural effusion presented a gradual and slower enhancement, due to inflammatory reaction and not due to the tumor extension (flare phenomenon) (Fig. 2). An open biopsy was performed and revealed an osteoblastoma. After surgical removal of the lytic lesion in the rib, the histopathological analysis confirmed an osteoblastoma with tumor-free margins, proving that the adjacent soft tissues edema and reactive pleural effusion occurred due to an inflammatory reaction (Fig. 3).

Discussion

Osteoblastomas are locally aggressive and intermediate-grade neoplasms that comprise 1–3% of all primary bone tumors [1]. Histologically, osteoblastomas are often undifferentiated from osteoid osteomas [2]. However, these tumors can be differentiated by the nidus size, while osteoblastoma has a nidus larger than 2 cm and osteoid osteoma has a nidus smaller than 2 cm [3]. Most osteoblastomas affect posterior elements of the vertebral column [2]. Its peak incidence is in the second decade of life, with a male predilection [1, 3]. The most commonly affected bones are the long tubular bones of the appendicular skeleton and vertebral bones. Tarsal bones, clavicle, and ribs are rarely involved [4]. Clinically, the patients may present with progressive pain, local swelling, and warmth not relieved by salicylates [5].

On radiograph and CT, osteoblastomas present as an expansive lytic lesion, with or without matrix mineralization, with a sclerotic rim, associated with periosteal reaction. Soft tissue tumor components may be present [3]. In a case series, 72% of osteoblastomas in the spine presented with matrix ossification, and in long tubular bones, 65% presented with matrix ossification, whereas, in the ribs, 50% had matrix ossification [6]. Usually, the periosteal reaction associated with osteoblastomas is solid or laminated, but can be spiculated [6].

On MRI, an osteoblastoma usually presents as an expansive bone lesion, with an intermediate or hypointense signal on T1-, variable signal on T2-weighted imaging, relative to skeletal muscles, and gadolinium enhancement

The case presentation can be found at https://doi.org/10.1007/s00256-023-04299-3

✉ Tatiana de Almeida Gonçalves Secco
tatiana.al1987@gmail.com

[1] Department of Radiology, Hospital Universitário Clementino Fraga Filho, Federal University of Rio de Janeiro, Rua Rodolpho Paulo Rocco 255, Cidade Universitária, Ilha do Fundão, Rio de Janeiro, RJ 21941-913, Brazil

[2] Department of Orthopedic Oncology, National Institute of Traumatology and Orthopedics, Av. Brasil, 500, Caju, Rio de Janeiro, RJ 20940-070, Brazil

[3] Department of Radiology, Clínica de Diagnóstico por Imagem (CDPI), Avenida das Américas, 4666, 302A, 303, 307, 325, 326, Barra da Tijuca, Rio de Janeiro, RJ 2640-102, Brazil

[4] Department of Radiology, Federal Fluminense University, Rua Marquês de Paraná, 303, Centro, Niterói, RJ 24070-035, Brazil

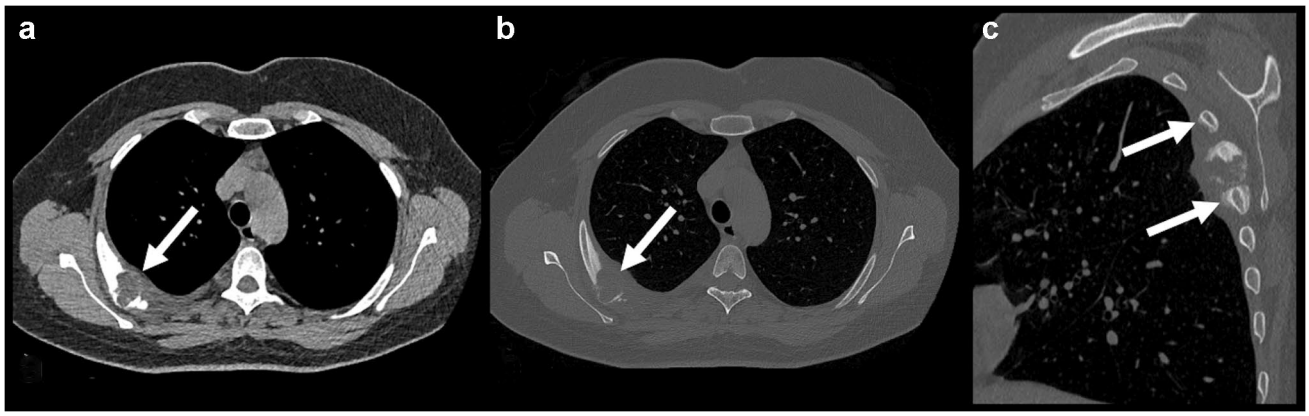

Fig. 1 Right fourth rib osteoblastoma. Chest CT demonstrated an expansile lytic lesion in the posterior portion of the right fourth rib, in the mediastinal (arrow in **a**) and bone windows (arrow in **b**), causing cortical erosion, with extension to the adjacent soft tissues, associated with a lamellar, solid, and concentric periosteal reaction and pleural effusion. Also note the reactive periosteal reaction in the adjacent third and fifth ribs, seen in the oblique sagittal plane, in the bone window (arrows in **c**)

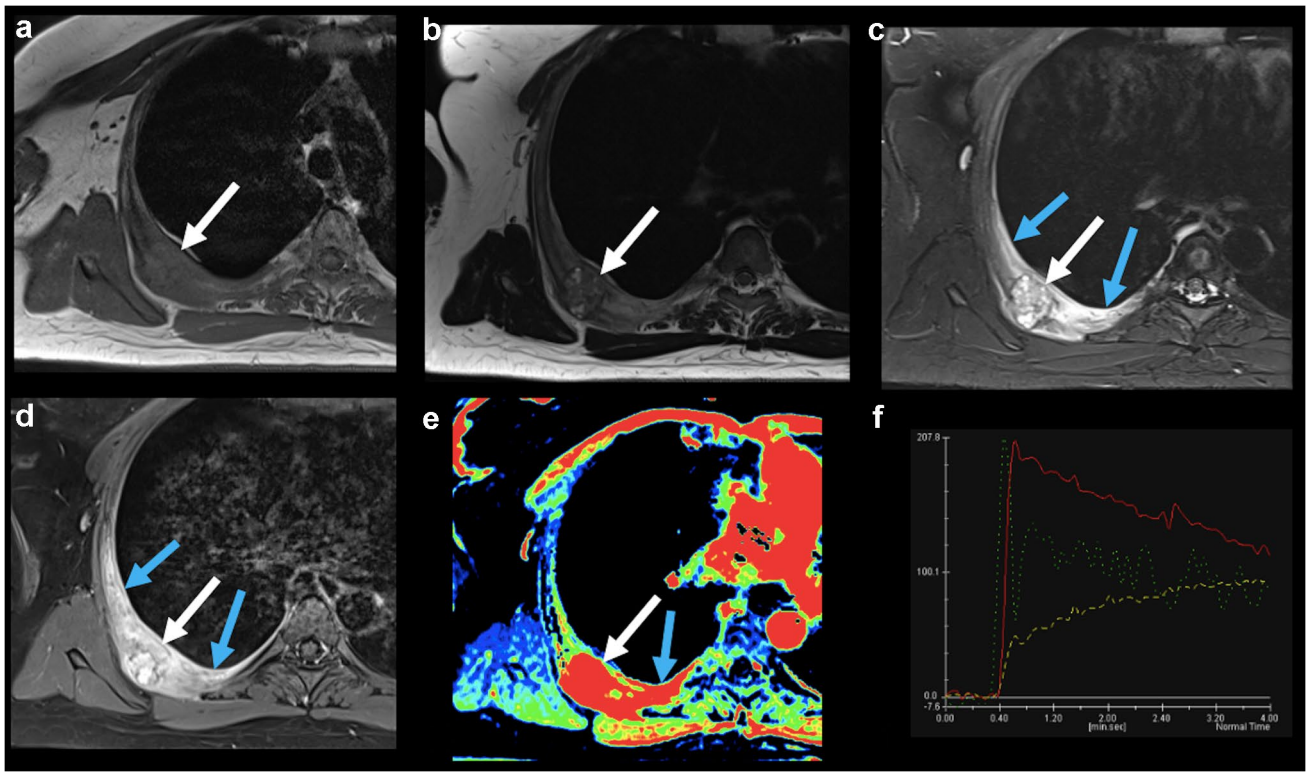

Fig. 2 Right fourth rib osteoblastoma. Chest MRI demonstrated an expansile intramedullary lesion in the posterior portion of the right fourth rib, with an isointense signal on T1- (arrow in **a**), predominantly hypointense signal on T2-weighted imaging (arrow in **b**), hyperintense signal on STIR (white arrow in **c**), relative to skeletal muscles, associated with avid gadolinium enhancement on T1-weighted imaging with fat saturation (white arrow in **d**). Note that there was extensive edema in the adjacent bone marrow and soft tissues, as well as reactive pleural effusion (blue arrows in **c**), which also presented avid gadolinium enhancement (blue arrows in **d**). Color-coded semi-quantitative dynamic contrast-enhanced (DCE) perfusion-weighted imaging map showed areas of high perfusion in the lesion (white arrow in **e**), as well as in the adjacent bone marrow, soft tissues, and reactive pleural effusion (blue arrow in **e**). However, the time-signal intensity curve analysis demonstrated that the lesion presented an early, intense, and rapid enhancement, with washout (red curve in **f**), due to tumor neoangiogenesis, whereas the adjacent soft tissues edema and reactive pleural effusion presented a gradual and slower enhancement (yellow curve in **f**), due to inflammatory reaction (flare phenomenon) and not due the tumor extension. The green curve in (**f**) in from the descending aorta, for comparison

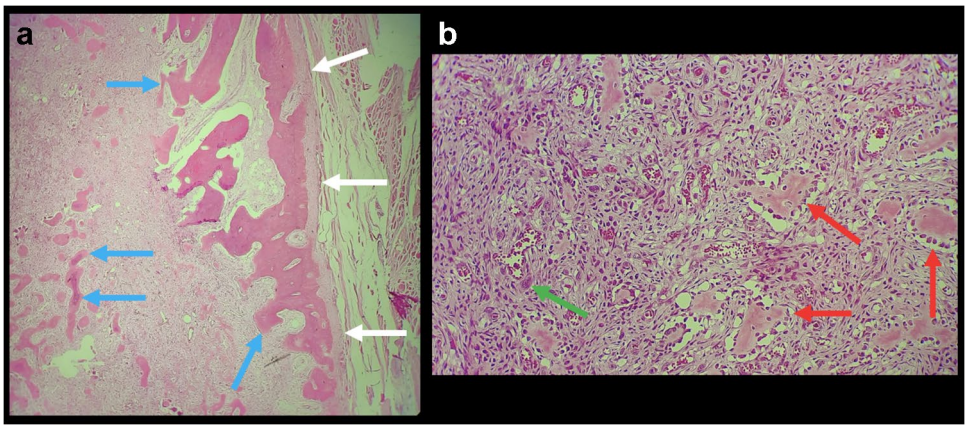

Fig. 3 Histopathological examination diagnostic of osteoblastoma. **a** Hematoxylin and eosin staining (original magnification, 40×) demonstrated a tumor with a well-defined border (white arrows in **a**), composed of interanastomosing trabeculae of woven bone (blue arrows in **b**) within a fibrovascular stroma. **b** Hematoxylin and eosin staining (original magnification, 200×) demonstrated that the osseous trabeculae are lined by a single layer of osteoblasts (red arrows in **b**). Also note the presence of an osteoclast type, multinucleated giant cell (green arrow in **b**)

[3, 7, 8]. Positron emission tomography with 2-deoxy-2-[fluorine-18]fluoro-D-glucose integrated with computed tomography (18-FDG PET-CT) shows a nodular lesion with intense uptake, with a maximum standard uptake value (SUVmax) of 12.3–16.0 [3].

Flare phenomenon is an inflammatory reaction, presenting as bone marrow edema, periosteal reaction, and soft-tissue edema surrounding the tumor [3]. This peritumoral inflammation associated with osteoblastoma was first described on MRI in 1990 [9]. On immunohistochemical analysis, positivity for cyclooxygenase-1 and -2 is seen in patients with this phenomenon, indicating that the neoplasm activates the arachidonic acid metabolic pathway, producing prostaglandin [1]. Then, it is hypothesized that prostaglandin production by the tumor can lead to the aggressive appearance on MRI, with peritumoral bone marrow edema, multifocal periostitis, soft tissue swelling, articular facet hypertrophy, and gadolinium enhancement that can completely resolve after the tumor is surgically resected [7].

Therefore, the flare phenomenon may lead to misinterpretation of the MRI, especially if the CT or radiograph features are not considered. The presence of bone marrow and soft tissue edema with gadolinium enhancement can lead to the consideration of a malignant tumor, such as osteosarcoma or Ewing sarcoma [2, 3].

Dynamic contrast-enhanced MRI may be useful to distinguish the tumor nidus from the peritumoral edema occurring due to the flare phenomenon. Tumor nidus demonstrates an early, intense, and rapid enhancement, with washout, seen on the time-signal intensity curve graph, due to tumor neoangiogenesis. Peritumoral edema presents a gradual and slower enhancement, due to inflammatory reaction (flare phenomenon), with an enhancement curve with a 20% slope or less, in comparison with the adjacent tumor [5].

It is important to consider the difference between the flare phenomenon related with osteoblastoma, which occurs before treatment, from the also-called flare phenomenon, related with an initial apparent deterioration of some bone metastasis or detection of novel lesions on imaging exams of patients with prostate cancer, after chemotherapy treatment initiation [10].

The main differential diagnosis of a lesion with aggressive characteristics in a rib in a young patient includes chondrosarcoma, osteosarcoma, and lymphoma. Chondrosarcomas usually appear in the costochondral or costovertebral junctions, with calcified rings-and-arcs matrix [5, 11]. Osteosarcomas occur in the costochondral junction, with a dense-ossified matrix, with internal hemorrhage and necrosis associated with a sunburst periosteal reaction. Chest wall lymphoma typically appears in the rib body, with a permeative appearance, with lamellated periosteal reaction, and restricted diffusion [11]. Fibrous dysplasia is commonly seen in the ribs, but it has non-aggressive characteristics, with a ground-glass appearance on CT, which did not occur in the presented case [11]. Furthermore, none of these lesions present with the flare phenomenon.

In conclusion, this case demonstrated that the flare phenomenon should be considered in the interpretation of imaging exams of patients with osteoblastoma. The performance of perfusion-weighted imaging with the analysis of the time-signal intensity curve pattern can be an important tool for the correct diagnosis of several bone tumors.

Declarations

Ethics approval All procedures performed in studies involving human participants were in accordance with the ethical standards of the institutional and national research committee and with the 1964 Helsinki Declaration and its later amendments or comparable ethical standards.

Informed consent Informed consent was obtained from the participant included in the study.

Animal rights This article does not contain any studies with animal subjects performed by any of the authors.

Conflict of interest The authors declare no competing interests.

References

1. Batra V, Batta NS, Gupta A. Toxic flare phenomenon in osteoblastoma: a case report with literature review. Indian J Musculoskelet Radiol. 2021;3(2):106–10.
2. Galgano MA, Goulart CR, Iwenofu H, Chin LS, Lavelle W, Mendel E. Osteoblastomas of the spine: a comprehensive review. Neurosurg Focus. 2016;41(2):E4. https://doi.org/10.3171/2016.5.FOCUS16122.
3. Huang Z, Fang T, Si Z, Li Y, Zhang L, Zheng C, et al. Imaging algorithm and multimodality evaluation of spinal osteoblastoma. BMC Musculoskelet Disord. 2020;21(1):240. https://doi.org/10.1186/s12891-020-03252-y.
4. Taghipour Zahir S, Sefidrokh Sharahjin N, Kargar S. A rare case of rib osteoblastoma: imaging features and review of literature. Iran J Radiol. 2013;10(3):152–5. https://doi.org/10.5812/iranjradiol.7108.
5. James SL, Panicek DM, Davies AM. Bone marrow oedema associated with benign and malignant bone tumours. Eur J Radiol. 2008;67(1):11–21. https://doi.org/10.1016/j.ejrad.2008.01.052.
6. Kroon HM, Schurmans J. Osteoblastoma: clinical and radiologic findings in 98 new cases. Radiology. 1990;175(3):783–90. https://doi.org/10.1148/radiology.175.3.2343130.
7. Chakrapani SD, Grim K, Kaimaktchiev V, Anderson JC. Osteoblastoma of the spine with discordant magnetic resonance imaging and computed tomography imaging features in a child. Spine (Phila Pa 1976). 2008;33(25):E968–70. https://doi.org/10.1097/BRS.0b013e31818a0271.
8. Shaikh MI, Saifuddin A, Pringle J, Natali C, Sherazi Z. Spinal osteoblastoma: CT and MR imaging with pathological correlation. Skeletal Radiol. 1999;28(1):33–40. https://doi.org/10.1007/s002560050469.
9. Crim JR, Mirra JM, Eckardt JJ, Seeger LL. Widespread inflammatory response to osteoblastoma: the flare phenomenon. Radiology. 1990;177(3):835–6. https://doi.org/10.1148/radiology.177.3.2243998.
10. Conteduca V, Poti G, Caroli P, Russi S, Brighi N, Lolli C, et al. Flare phenomenon in prostate cancer: recent evidence on new drugs and next generation imaging. Ther Adv Med Oncol. 2021;13:1758835920987654. https://doi.org/10.1177/1758835920987654.
11. Goldbach AR, Kumaran M, Donuru A, McClure K, Dass C, Hota P. The spectrum of rib neoplasms in adults: a practical approach and multimodal imaging review. AJR Am J Roentgenol. 2020;215(1):165–77. https://doi.org/10.2214/AJR.19.21554.